Paper 5758-44, to be published in the Proceedings of the SPIE Smart Structures Conference
*San Diego, CA., Mar 6-10. 2005, SPIE Vol. **5758***

Efficient Electromechanical Network Models for Wireless Acoustic-Electric Feed-throughs

Stewart Sherrit, Mircea Badescu, Xiaoqi Bao, Yoseph Bar-Cohen, Zensheu Chang
Jet Propulsion Laboratory, California Institute of Technology, Pasadena, CA

ABSTRACT

There are numerous engineering design problems where the use of wires to transfer power and communicate data thru the walls of a structure is prohibitive or significantly difficult that it may require a complex design. Such systems may be concerned with the leakage of chemicals or gasses, loss of pressure or vacuum, as well as difficulties in providing adequate thermal or electrical insulation. Moreover, feeding wires thru a wall of a structure reduces the strength of the structure and makes the structure susceptibility to cracking due to fatigue that can result from cyclic loading. Two areas have already been identified to require a wireless alternative capability and they include (a) the container of the Mars Sample Return Mission will need the use of wireless sensors to sense pressure leak and to avoid potential contamination; and (b) the Navy is seeking the capability to communicate with the crew or the instrumentation inside marine structures without the use of wires that will weaken the structure. The idea of using elastic or acoustic waves to transfer power was suggested recently by Y. Hu, et al.[1]. However, the disclosed model was developed directly from the wave equation and the linear equations of piezoelectricity. This model restricted by an inability to incorporate head and tail mass and account for loss in all the mechanisms. In addition there is no mechanism for connecting the model to actual power processing circuitry (diode bridge, capacitors, rectifiers etc.). An alternative approach which is to be presented is a network equivalent circuit that can easily be modified to account for additional acoustic elements and connected directly to other networks or circuits. All the possible loss mechanisms of the disclosed solution can be accounted for and introduced into the model. The circuit model allows for both power and data transmission in the forward and reverse directions through acoustic signals at the harmonic and higher order resonances. This system allows or the avoidance of cabling or wiring. The technology is applicable to the transfer of power for actuation, sensing and other tasks inside sealed containers and vacuum/pressure vessels.

Keywords: Ultrasonic, Bulk Acoustic Waves, power conversion, isolation, pressure vessels

1. INTRODUCTION-THEORY

A variety of situations exist where power or information is required to be transmitted across a physical barrier without perforating the barrier. If the barrier material is thin or transparent to electromagnetic waves in the frequency of interest this can be accomplished optically or with magnetic coupling. If this is not the case then other means are required to accomplish this task. The idea of using elastic or acoustic waves as to transfer power was suggested recently by Y. Hu, et al.[1] In the system they investigated a transmit and receive piezoelectric transducer were separated by a sealed armor (wall). A sinusoidal voltage was applied across the transmit piezoelectric at a known frequency generating an acoustic wave that travel through the armor into the receive piezoelectric where the stress wave generated a sinusoidal voltage. Useful work was done on a load impedance connected electrically in parallel with the receive piezoelectric. A similar configuration to the one they described is shown schematically in Figure 1. In the configuration shown a front and tail mass have been added to the system in an effort to increase the design variables. In the work of Hu et. al [1] the piezoelectric/elastic layer/piezoelectric was solved using the wave equation and linear equations of piezoelectricity and constant stress boundary condition between the layers and traction free surfaces. An alternative approach based on network equivalent circuits[2,3] that can easily be modified to account for additional acoustic elements and connected directly to other networks or circuits. All the possible loss mechanisms of the solution can be accounted for and introduced into the model. The circuit model allows for both power and data transmission in the forward and reverse directions through acoustic signals at the harmonic and higher order resonances. This system allows for the avoidance of cabling or wiring. The technology is applicable to the transfer of power for actuation, sensing data or other tasks inside sealed containers and vacuum/pressure vessels. A schematic diagram of the model for the system shown in Figure 1 is shown in Figure 2.

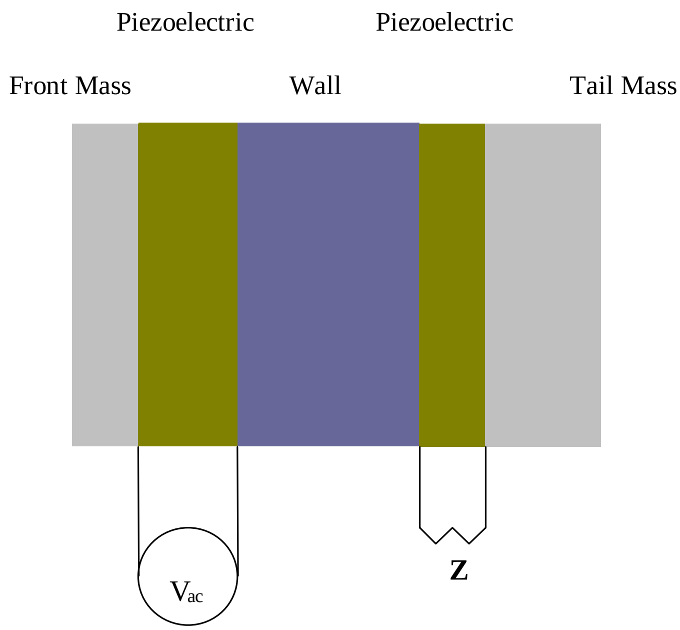

Figure 1. Schematic of the physical acoustic-electric system with a piezoelectric generator and receiver. The tail and front mass are optional. The delivered power is consumed in the impedance **Z**

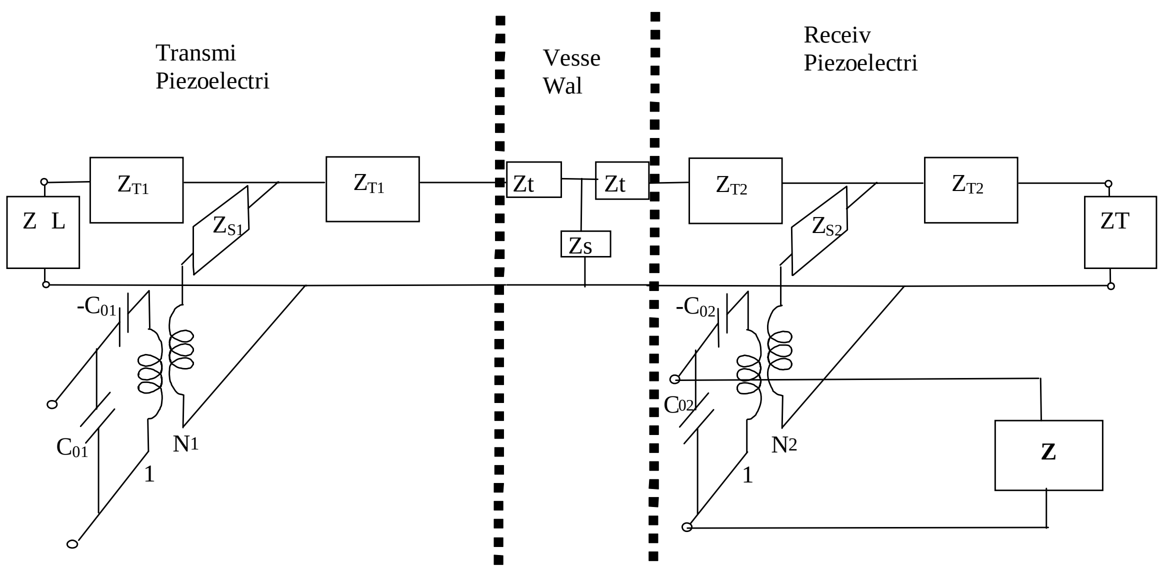

Figure 2. Schematic of the network equivalent circuit for the physical system shown in Figure 1. The delivered power is consumed in the impedance **Z**. ZTL and ZTR are the terminating mechanical impedances associated with the front and tail mass.

The model parameters for the network circuit shown in Figure 2 are listed in Table 1. These models have been widely used for backed/matched and mass loaded resonators[4], transient response[5], material constant determination[6], and a host of other applications[7]. One of the perceived problems with the model is that it required a negative capacitance at the electrical port. Although Redwood[5] showed that this capacitance could be transformed to the acoustic side of the transformer and treated like a length of the acoustic line it was still thought to be "un-physical".

Table 1. The coefficients and model parameters of the network equivalent shown in Figure 2.

Material Properties
$\boldsymbol{\varepsilon}_{33}^{S}$ clamped complex permittivity
$\mathbf{c}_{33}^{D}$ open circuit complex elastic stiffness
$\boldsymbol{k}_t$ complex electromechanical coupling
$\boldsymbol{k}_t^2 = \boldsymbol{e}_{33}^2 / \mathbf{c}_{33}^{D}\boldsymbol{\varepsilon}_{33}^{S} = \boldsymbol{h}_{33}^2\boldsymbol{\varepsilon}_{33}^{S} / \mathbf{c}_{33}^{D}$
$\boldsymbol{h}_{33} = \boldsymbol{k}_t\sqrt{\mathbf{c}_{33}^{D} / \boldsymbol{\varepsilon}_{33}^{S}}$
Mason's Model (Generator) ρ=density, t= thickness, A=area
$\mathbf{C}_{01} = \dfrac{\boldsymbol{\varepsilon}_{33_1}^{S} A_1}{t_1}$ $\qquad \mathbf{N}_1 = \mathbf{C}_{01}\boldsymbol{h}_{33_1}$
$\mathbf{Z}_{01} = \rho_1 A_1 \mathbf{v}_1^{\mathbf{D}} = A_1\sqrt{\rho_1 \mathbf{c}_{33_1}^{D}}$ $\qquad \boldsymbol{\Gamma}_1 = \dfrac{\omega}{\mathbf{v}_1^{\mathbf{D}}} = \omega\sqrt{\dfrac{\rho_1}{\boldsymbol{c}_{33_1}^{D}}}$
$Z_{T1} = i\mathbf{Z}_{01}\tan(\boldsymbol{\Gamma}_1 t_1/2)$ $\qquad Z_{S1} = -i\mathbf{Z}_{01}\csc(\boldsymbol{\Gamma}_1 t_1)$
Mason's Model (Reciever) ρ=density, t= thickness, A=area
$\mathbf{C}_{02} = \dfrac{\boldsymbol{\varepsilon}_{33_2}^{S} A_2}{t_2}$ $\qquad \mathbf{N}_2 = \mathbf{C}_{02}\boldsymbol{h}_{33_2}$
$\mathbf{Z}_{02} = \rho_2 A_2 \mathbf{v}_2^{\mathbf{D}} = A_2\sqrt{\rho_2 \mathbf{c}_{33_2}^{D}}$ $\qquad \boldsymbol{\Gamma}_2 = \dfrac{\omega}{\mathbf{v}_2^{\mathbf{D}}} = \omega\sqrt{\dfrac{\rho_2}{\boldsymbol{c}_{33_2}^{D}}}$
$Z_{T2} = i\mathbf{Z}_{02}\tan(\boldsymbol{\Gamma}_2 t_2/2)$ $\qquad Z_{S2} = -i\mathbf{Z}_{02}\csc(\boldsymbol{\Gamma}_2 t_2)$
Wall Properties ρ=density, t= thickness, A=area
$Z_{tw} = i\mathbf{Z}_w\tan(\boldsymbol{\Gamma}_w t_w/2)$ $\qquad Z_{sw} = -i\mathbf{Z}_w\csc(\boldsymbol{\Gamma}_w t_w)$
$\mathbf{Z}_w = \rho_w A_w \mathbf{v}_w^{\mathbf{D}} = A_w\sqrt{\rho_w \mathbf{c}_w^{D}}$ $\qquad \boldsymbol{\Gamma}_w = \dfrac{\omega}{\mathbf{v}_w^{\mathbf{D}}} = \omega\sqrt{\dfrac{\rho_w}{\boldsymbol{c}_w^{D}}}$
Tail mass properties ρ=density, t= thickness, A=area
$Z_{TR} = i\mathbf{Z}_R\tan(\boldsymbol{\Gamma}_R t_R)$ termination impedance
$\mathbf{Z}_R = \rho_R A_R \mathbf{v}_R^{\mathbf{D}} = A_R\sqrt{\rho_R \mathbf{c}_R^{D}}$ $\qquad \boldsymbol{\Gamma}_R = \dfrac{\omega}{\mathbf{v}_R^{\mathbf{D}}} = \omega\sqrt{\dfrac{\rho_R}{\boldsymbol{c}_R^{D}}}$
Head Mass properties ρ=density, t= thickness, A=area
$Z_{TL} = i\mathbf{Z}_L\tan(\boldsymbol{\Gamma}_L t_L)$ termination impedance
$\mathbf{Z}_L = \rho_L A_L \mathbf{v}_L^{\mathbf{D}} = A_L\sqrt{\rho_L \mathbf{c}_L^{D}}$ $\qquad \boldsymbol{\Gamma}_L = \dfrac{\omega}{\mathbf{v}_L^{\mathbf{D}}} = \omega\sqrt{\dfrac{\rho_L}{\boldsymbol{c}_L^{D}}}$
Load Impedance = **Z**

In an effort to remove circuit elements between the top of the transformer and the node of the acoustic transmission line Krimholtz, Leedom and Matthae[8] published an alternative equivalent circuit. This model is commonly referred to as the KLM model and has been used extensively in the medical imaging community in an effort to design high frequency transducers [9,10], multilayers[11], and arrays[12]. In previous work we have shown that the KLM and the Mason's equivalent network models produced results identical with the solution to the wave equation in layered structures[2] if the loss was treated in a similar fashion for each model. The configuration shown in Figure 2 is also applicable to voltage transformers where the stress distribution is amplified in the output transducer due to the mechanical Q's to produce larger voltages. The solution to the model proceeds as with any network solution. In this representation the voltage on the mechanical side of a transformer corresponds with the force and the current corresponds with the velocity of the surface. Voltage is multiplied by the transformer ratio N when moving from the electrical to mechanical side of the transformer while the current is divided by N. When moving from the mechanical side to the electrical side the voltage is divided by the transformer ratio N and the current is multiplied by N. The resulting impedances starting at the load impedance on the receive transducer and working to the left are;

$$Zx1 = \mathbf{Z}\frac{Z02}{\mathbf{Z} + Z02}, \tag{1}$$

$$Zx2 = Zx1 - Z02, \tag{2}$$

$$Zx3 = N_2^2 Zx2 \quad , \tag{3}$$

$$Zx4 = Zs2 + Zx3, \tag{4}$$

$$Zx5 = Zx4\frac{(Zt2 + ZtR)}{(Zt2 + ZtR + Zx4)}, \tag{5}$$

$$Zx6 = Zx5 + Zt2 + Ztw, \tag{6}$$

$$Zx7 = Zx6\frac{Zsw}{Zx6 + Zsw}, \tag{7}$$

$$Zx8 = Zx7 + Ztw + Zt1 \quad , \tag{8}$$

$$Zx9 = Zx8\frac{(Zt1 + ZtL)}{(Zx8 + Zt1 + ZtL)} \quad , \tag{9}$$

$$Zx10 = Zs1 + Zx9 \quad , \tag{10}$$

$$Zx11 = \frac{Zx10}{N_1^2}, \tag{11}$$

$$Zx12 = Zx11 - Z01, \tag{12}$$

$$Zx13 = Zx12\frac{Z01}{(Zx12 + Z01)} \quad , \tag{13}$$

where Zx13 is the input impedance as seen from the electrical port of the transmit piezoelectric. From the impedances shown in equations (1) to (13) and the applied voltages we can calculate the current in the various branches of the circuit in Figure 2. In the following discussion we use V for a sinusoidal input $V = V_0\sin(\omega t)$. The impedance values are in general complex and we note that dividing or multiplying by a complex value implies a change in both the magnitude and the phase of the signal. The current through the electrical port of the transmit piezoelectric is therefore

$$I = V / Zx13. \tag{14}$$

The current through the transformer on the electrical side of the transmit piezoelectric is

$$I2 = I\frac{Z01}{(Z01 + Zx2)}. \tag{15}$$

The velocity (current) through the transformer on the mechanical side is

$$v3 = \frac{I2}{N1}. \tag{16}$$

The velocity (current) of the left face of the wall is

$$v4 = v3\frac{Zt1 + ZtL}{Zt1 + ZtL + Zx8}. \tag{17}$$

The velocity (current) at the right face of the wall is

$$v5 = v4\frac{Zs0}{Zs0 + Zx6}\quad. \tag{18}$$

The velocity (current) into the mechanical side of the receive transformer of the piezoelectric is

$$v6 = v5\frac{Zt2 + ZtR}{Zt2 + ZtR + Zx4}\quad. \tag{19}$$

The current through the electrical side of the transformer for the receive piezoelectric is

$$I7 = v6N2. \tag{20}$$

The current through the load resistor is

$$I_L = I7\frac{Z02}{Z02 + \mathbf{Z}}\quad. \tag{21}$$

The Voltage across the load resistor is

$$V_L = I_L\mathbf{Z}. \tag{22}$$

The power delivered to the load resistor is

$$P_L = \mathrm{Re}(V_L I_L)\ , \tag{23}$$

and the power efficiency of the acoustic electrical feed-through is therefore

$$\eta_L = \frac{\mathrm{Re}(V_L I_L)}{\mathrm{Re}(VI)}\quad. \tag{24}$$

The voltage gain is

$$\alpha_V = |V_L|/|V|\ . \tag{25}$$

In order to test the validity of the model compared to the solution calculated directly from the wave equation[1] we have used the material properties used by Hu et al. to calculate the efficiency ,input impedance, voltage gain and power. The material properties used and the geometry are shown in Table 2.

Table 2. Data used by Hu et al.[1] to calculate response of the power transfer efficiency. The transmit and receive piezoelectric transducers were of the same material and head and tail masses were not used.

Property	Value
Density of Piezoelectric (kg/m^3)	7500
Density of wall (kg/m^3)	7850
Area of piezoelectric on wall (m^2)	0.01
Wall thickness (m)	0.006
Transmit Piezoelectric thickness (m)	0.002
Receive Piezoelectric thickness (m)	0.001
Piezoelectric Coefficient e_{33} (C/m^2)	23.3
Permittivity (F/m) ε^S_{33}	1.302x10^{-8}
Elastic stiffness at constant Field c^E_{33} (N/m^2)	11.7x10^{10} (1+0.01i)
Thickness Coupling	0.513(1-0.00368i)
Elastic stiffness at constant Displacement c^D_{33} (N/m^2)	15.87x10^{10}(1+0.00737i)
Elastic stiffness of wall c_w (N/m^2)	26.9x10^{10}(1+0.01i)

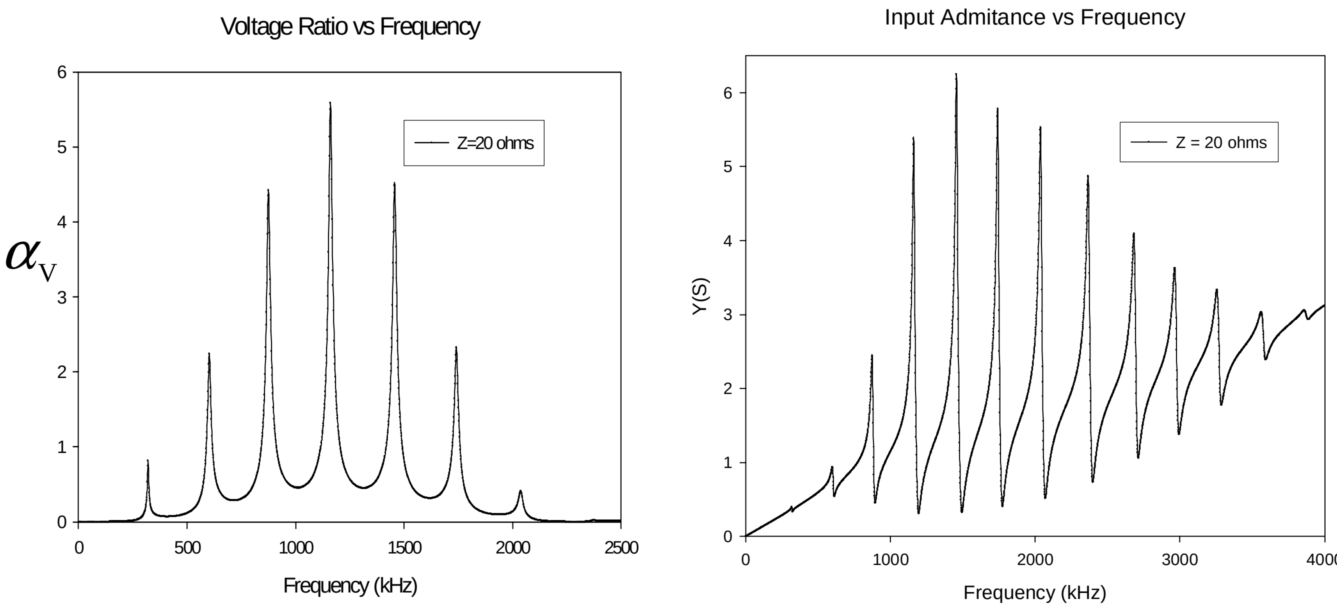

Figure 3. The voltage ratio and input impedance based on the input data and geometry published by Hu et al.[1] using the electromechanical model discussed in this paper. The curves are identical to data that was published by Hu et al. which was based on solving the wave equation directly.

The efficiency for a variety of load impedances is shown in Figure 4. The maximum efficiency for this design is 82.5 percent at Z_L =3 ohms .

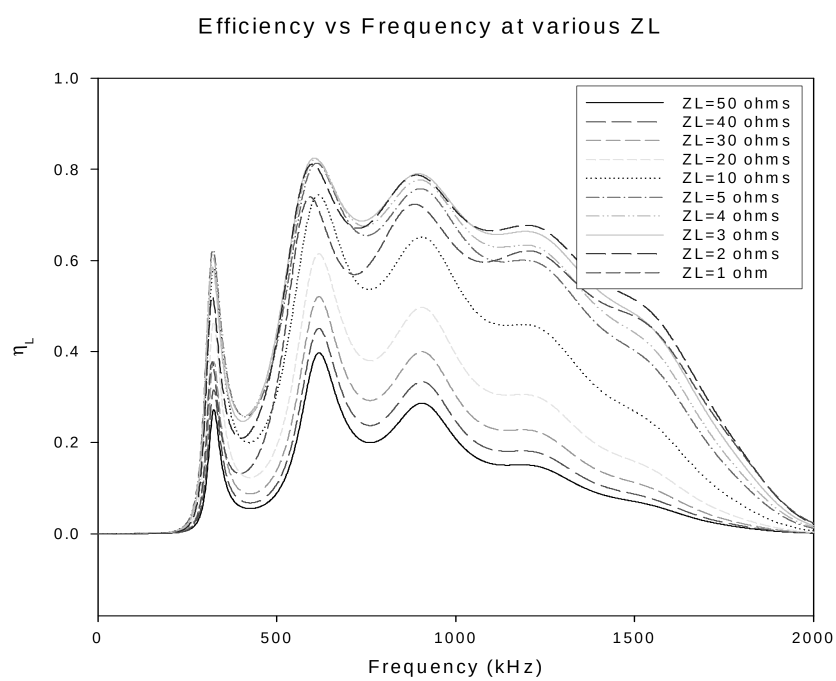

Figure 4. The efficiency of the power transfer for the acoustic electric feed-through described by Hu et al.[1] as a function of the frequency. Maximum efficiency is about 82.5% at Z_L= 3 ohms at 650kHz.

2. APPLICATION OF LOSS

It is apparent that assuming that the wall and piezoelectric have the same mechanical Q or loss factor may not be a reasonable approximation for a comparison with a real system. In addition ignoring both the dielectric loss and piezoelectric loss can introduce errors and may limit the usefulness of a practical device. In order to investigate the actual loss on the device we have recalculated the input impedance based on material coefficients determined from thickness resonance data for a Motorola 3203HD material with similar properties to the 5H material discussed by Hu et.al.[1]

Table 3. Data used to study the acoustic-electric feedthrough with measured coefficients for the piezoelectric (Motorola 3203HD – now CTS Wireless Products). This material is a soft PZT with similar nominal properties to 5H. The transmit and receive piezoelectric transducers were of the same material and head and tail masses were not used.

Property	Value
Density of Piezoelectric (kg/m^3)	7850
Density of wall (kg/m^3)	7850
Area of piezoelectric on wall (m^2)	0.01
Wall thickness (m)	0.006
Transmit Piezoelectric thickness (m)	0.002
Receive Piezoelectric thickness (m)	0.001
Piezoelectric Coefficient e_{33} (C/m^2)	23.38(1-0.03495i)
Permittivity (F/m) ε^S_{33}	1.061×10^{-8}(1-0.0485i)
Elastic stiffness at constant Field c^E_{33} (N/m^2)	12.28×10^{10} (1+0.0253i)
Thickness Coupling	0.5435(1-0.01649i)
Elastic stiffness at constant Displacement c^D_{33} (N/m^2)	17.43×10^{10}(1+0.0115i)
Elastic stiffness of wall c_w (N/m^2)	26.9×10^{10}(1+0.01i)

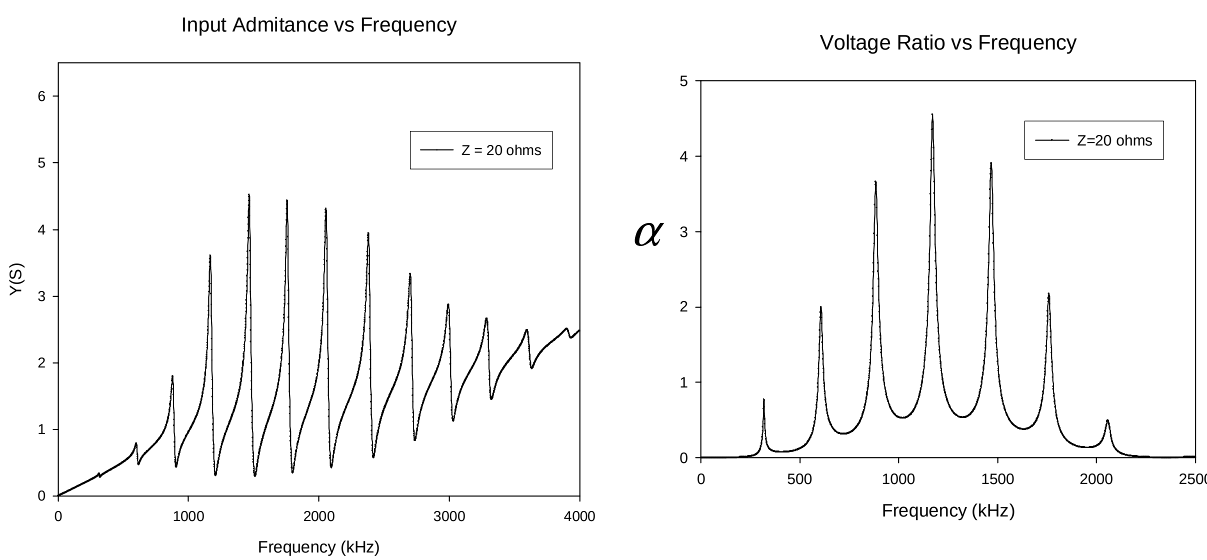

Figure 5. Input admittance and voltage ratio of the device with measured material constants shown in Table 3. The output piezoelectric is shunted by a 20 ohm load impedance.

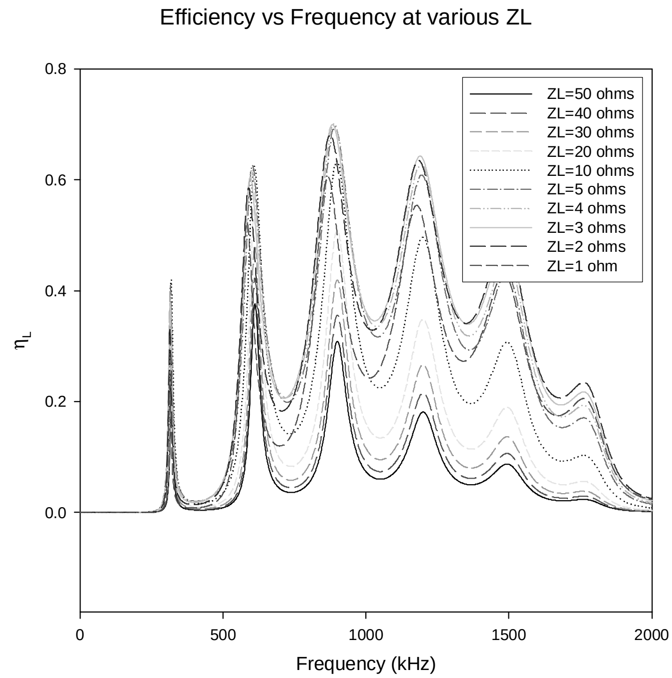

Figure 6: The efficiency for the acoustic electric transformer using the measured material constants shown in Table 3.

It is apparent from the data shown in Figures 5 and 6 compared to the data in Figures 3 and 4 that the change in both the input impedance and the voltage ratio is small however a noticeable change in the efficiency is found especially away from the peaks in the curves. These results although they include loss represent a best case in that we have not modeled the effect of the bond.

3. INVESTIGATION OF HARD PZT

In addition to the modeling of loss another aspect of these devices is that they will be used to transmit power and heating effects may become significant. PZT 5H is a soft PZT with large temperature dependence. In addition the onset of non-linearity occurs at drive fields that are much lower than the hard PZT's such as the NAVY I or III materials. In order to investigate that similar efficiencies can be achieved using NAVY III materials we have repeated the analysis above for small signal thickness material values determined experimentally for a Morgan Matroc Navy III material (PZT-8). The thickness data is shown in Table 4. along with the dimensions and density.

Table 4. Data used to study the acoustic-electric feedthrough with measured coefficients for the piezoelectric (Morgan Matroc PZT-8). This material is a hard PZT with similar nominal properties to Navy III. The transmit and receive piezoelectric transducers were of the same material and head and tail masses were not used.

Property	Value
Density of Piezoelectric (kg/m^3)	7750
Density of wall (kg/m^3)	7850
Area of piezoelectric on wall (m^2)	0.01
Wall thickness (m)	0.006
Transmit Piezoelectric thickness (m)	0.002
Receive Piezoelectric thickness (m)	0.001
Piezoelectric Coefficient e_{33} (C/m^2)	12.3(1+0.0015i)
Permittivity (F/m) ε^S_{33}	$6.16\text{x}10^{-9}$(1-0.003i)
Elastic stiffness at constant Field c^E_{33} (N/m^2)	$16.1\text{x}10^{10}$ (1+0.002i)
Thickness Coupling	0.364(1+0.00063i)
Elastic stiffness at constant Displacement c^D_{33} (N/m^2)	$18.6\text{x}10^{10}$(1+0.0025i)
Elastic stiffness of wall c_w (N/m^2)	$26.9\text{x}10^{10}$(1+0.01i)

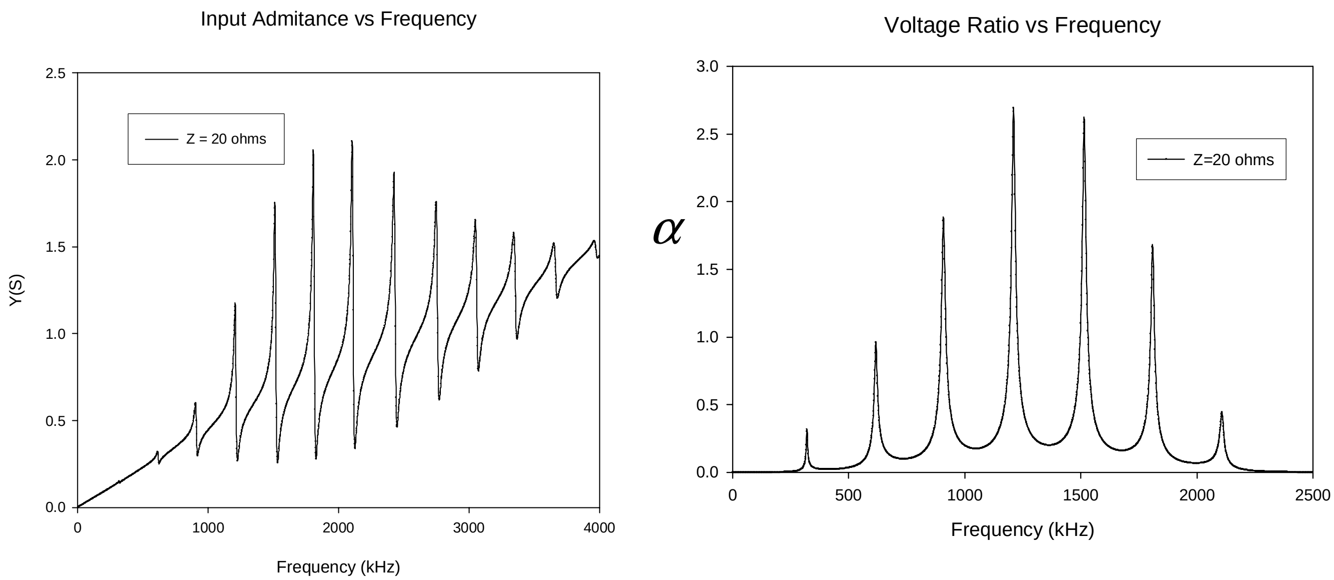

Figure 7. Input admittance and voltage ratio of the device with measured material constants (PZT-8) shown in Table 4. The output piezoelectric is shunted by a 20 ohm load impedance.

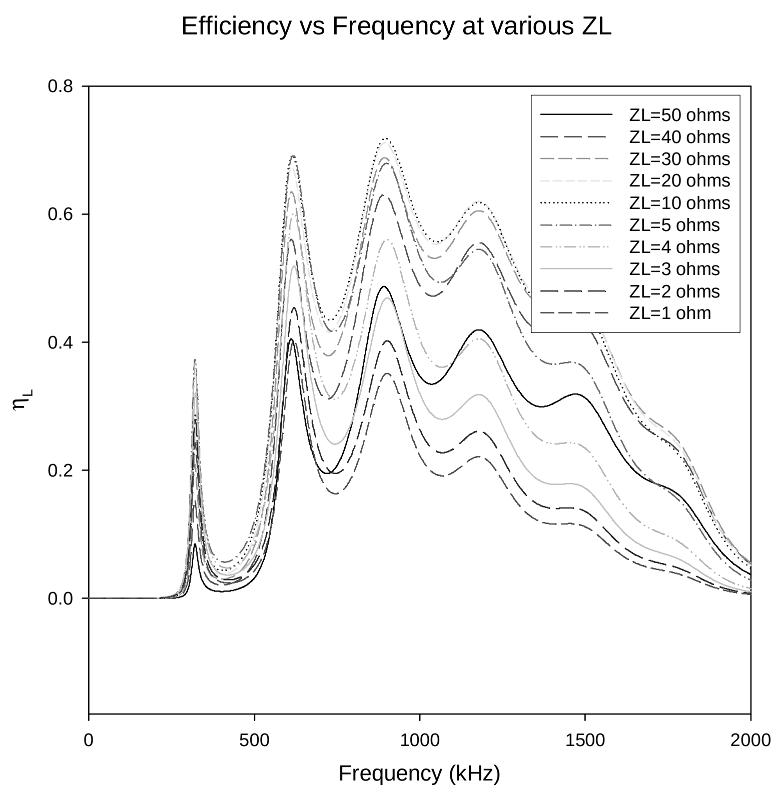

Figure 8. The efficiency as a function of the load impedance for the acoustic electric transformer using the measured material constants shown in Table 4.

It is interesting to note that using a Navy III material such as PZT-8 reduces the efficiency and voltage ratio. The maximum efficiency is approximately 70% at 1 MHz for a 10 ohm impedance. The efficiency and voltage ratio do not decrease as much away from the peaks as was the case for the modeling assuming dielectric or piezoelectric loss. This is likely due to the lower loss is PZT-8 compared to PZT 5H materials. It should be noted that by increasing the wall mechanical Q from 100 to 1000 pushes the efficiency above 90%. Another aspect the will be critical and that we are currently investigating is the bond material. In the case of high Q piezoelectric materials and high Q wall materials the limiting effect will likely occur in the bond. We are currently investigating a variety of bonding techniques including the use of epoxies, low temperature solders and bolting the piezoelectrics to the wall.

4. SUMMARY

A wireless acoustic electric feed-through network model was investigated and compared to models developed directly from the wave equation and the linear equations of piezoelectricity. The models were found to produce identical results when the same material parameters were used. The model was extended to include dielectric, piezoelectric and mechanical losses in the piezoelectric and mechanical loss in the wall. Simulations using material parameters with loss showed that the efficiency and voltage ratio were change primarily away from the peaks. Since the devices are primarily designed to transmit power the analysis was repeated on hard PZT. Again the results were similar and somewhat lower. Increasing the mechanical Q of the wall material for this case increased the efficiency which suggests that the efficiency is primarily controlled by model element with the largest mechanical loss which implies that the bonding material joining the piezoelectric and the wall will be critical to these devices.

ACKNOWLEDGEMENTS

The research described in this paper was carried out at the Jet Propulsion Laboratory, California Institute of Technology, under a contract with the National Aeronautics and Space Administration.

REFERENCES

1 Y. Hu, X. Zhang, J. Yang, Q. Jiang, " Transmitting Electric Energy Through a Metal Wall by Acoustic Waves Using Piezoelectric Transducers, IEEE Transactions on Ultrasonics, Ferroelectrics, and Frequency Control, **50**, 7, pp. 773-781, 2003

2 S. Sherrit, Y. Bar-Cohen, and X. Bao, "Efficient Electromechanical Network Model for Wireless Acoustic-Electric Feed-throughs (WAEF)," NASA New Technology Report, Docket No. **41157**, submitted on June 21, 2004.

3 S. Sherrit, S. P. Leary, B. P. Dolgin and Y. Bar-Cohen, "Comparison of the Mason and KLM Equivalent Circuits for Piezoelectric Resonators in the Thickness Mode", Proceedings of the IEEE Ultrasonics Symposium, Lake Tahoe, 1999, pp. 921-926

4 D. A. Berlincourt, D.R. Curran, H. Jaffe, "Chapter 3- Piezoelectric and Piezomagnetic Material and their Function in Transducers, pp. 169-270, <u>Physical Acoustics-*Principles and Methods*</u>, Volume 1-Part A, ed. W.P. Mason Academic Press, New York, 1964

5 M. Redwood, “Transient Performance of a Piezoelectric Transducer”, Journal of the Acoustical Society of America, **33**, pp.527-536, 1961

6 S. Saitoh, H Honda, N. Kaneko, M. Izumi, S. Suzuki, The Method of Determining k_t and Q_m for low Q piezoelectric materials” Proceedings of the IEEE Symposium on Ultrasonics, San Francisco, CA, pp. 620-623, 1985

7 <u>Solid State Magnetic and Dielectric Devices</u>, edited by H.W. Katz, John Wiley and Sons, New York , 1959

8 R. Krimholtz, D.A. Leedom, G.L. Matthaei, “New Equivalent Circuit for Elementary Piezoelectric Transducers”, Electron Letters, Electron. Lett. **6**, pp. 398-399,1970

9 M. J. Zipparo, K.K. Shung, T.S. Shrout, “Piezoceramics for High Frequency (20-100 MHz) Single Element Imaging Transducers”, IEEE Trans on Ultrasonics, Ferroelectrics and Frequency Control, **44**, pp.1038-1048, 1997

10 F.S. Foster, L.K. Ryan, D.H. Turnbull, “Characterization of Lead Zirconate Titanate Ceramics for Use in Miniature High Frequency (20-80 MHz) Transducers, IEEE Trans on Ultrasonics, Ferroelectrics and Frequency Control , **38**, pp. 446-453, 1991

11 Q. Zhang, P.A. Lewin, P.E. Bloomfield, “PVDF Transducers- A Performance Comparison of Single-Layer and Multilayer Structures”, IEEE Trans on Ultrasonics, Ferroelectrics and Frequency Control, **44**, pp.1148-1156, 1997

12 R.L. Goldberg, M.J. Jurgens, D.M. Mills, C.S. Henriquez, D.Vaughan, S. W. Smith, “Modeling of Piezoelectric Multilayer Ceramics Using Finite Element Analysis”, IEEE Trans on Ultrasonics, Ferroelectrics and Frequency Control., **44**, pp. 1204-1214, 1997